Desalination and Water Treatment
www.deswater.com

doi: 10.5004/dwt.2020.26053

198 (2020) 98–107
September

A positively charged PI nanofiltration membrane with good separation for Li^+ and Mg^{2+}

Qiuyan Bi[a,b], Shiai Xu[a,b,*]

[a]*Shanghai Key Laboratory of Advanced Polymeric Materials, Key Laboratory for Ultrafine Materials of Ministry of Education, School of Materials Science and Engineering, East China University of Science and Technology, Shanghai 200237, China, Tel. +86 971 5310422; email: saxu@ecust.edu.cn (S. Xu), Tel. +86 21 64253353; email: bqy1110@163.com (Q. Bi)*
[b]*School of Chemical Engineering, Qinghai University, Xining 810016, China*

Received 3 November 2019; Accepted 3 May 2020

ABSTRACT

A positively charged PI/PDA/PEI nanofiltration membrane was prepared in this study by cross-linking between polyethyleneimine (PEI) and poly(dopamine) (PDA) on the polyimide (PI) support membrane for separating Mg^{2+} and Li^+ from $MgCl_2$/LiCl mixed solution, and its chemical structure, surface properties, and separation performance were investigated. The results indicate that the PI/PDA/PEI membrane has a thin positively charged layer and shows excellent rejections against many inorganic salts [$MgCl_2$ (93.1%) > $MgSO_4$ (86.5%) > Na_2SO_4 (74.7%) > LiCl (37.6%)]. More importantly, the membrane exhibits long-term stability and good separation of Mg^{2+} and Li^+, and the Mg/Li ratio of the permeate of brine obtained from West Taijnar salt lake can be reduced from 65.3 to 5.0 at pH 6.5 by filtration.

Keywords: Nanofiltration; Cross-linking; Salt lake brine; High Mg/Li ratio

1. Introduction

Lithium (Li) has been widely used in various applications such as battery, nuclear power, aerospace, and alloys [1]. Many methods have been developed to separate Li^+ from brine with a high Mg/Li ratio, such as precipitation [2], extraction [3], ion exchange and sorption [4], and membrane separation [5]. Nanofiltration (NF) membrane can separate multivalent ions and small organic compounds with a molecular weight of 200–1,000 Da, and thus it has the potential to be used to recover Li^+ from salt lake brine without causing any environmental impacts [6–8]. Wen et al. [5] first reported the recovery of Li^+ from diluted salt lake brine using NF membrane, and the result showed that the separation factor (SF) of Li^+ and Mg^{2+} was about 3.5. Yang et al. [9] showed that the SF was 2.6 for simulated brine with an Mg/Li ratio of 24 at 1.0 MPa using a spiral-wound Desal DK membrane. Somrani et al. [10] showed that NF90 was better than the XLE membrane in separating Mg^{2+} and Li^+ from diluted Tunisian salt lake brine with an Mg/Li ratio of 50. Sun et al. [11] showed that the rejection of Mg^{2+} was 65% and the SF was about 3.3 for the simulated West Taijiner brine with an Mg/Li ratio of 64 at 3.0 MPa using Desal DL-2540 model.

However, it is important to note that almost all available NF membranes are negatively charged. According to Donnan exclusion theory, a positively charged NF membrane is more capable of separating Mg^{2+} and Li^+ than a negatively charged one. Li et al. [12] prepared a positively charged hollow fiber NF membrane by interfacial polymerization (IP) of 1,4-bis(3-aminopropyl)-piperazine and trimesoyl chloride (TMC) on polyacrylonitrile ultrafiltration membranes for the separation of Mg^{2+} and Li^+, and the results showed that the Mg/Li ratio decreased from 20 to 7.7 after filtration by the composite membrane and the SF of the composite membrane (2.6) was higher than that of commercial NF90 membrane (2.1). Li et al. [13] synthesized a positively

* Corresponding author.

charged NF membrane by IP of branched polyethyleneimine (PEI) and TMC followed by modification of ethylene diamine tetraacetic acid disodium salt on polyetherimide support membrane, and this NF membrane showed good stability and an SF about 9.2 for $MgCl_2$/LiCl mixed solution with an Mg/Li ratio of 24. Zhang et al. [14] fabricated a positively charged NF membrane by IP using PEI as aqueous precursor and TMC as an organic monomer, and the modified multi-walled carbon nanotubes with hydroxyl groups were added to the aqueous solution to enhance the permeability of the membrane. The fabricated membrane showed the potential to recover Li^+ from mixed salt solution or seawater with a high Mg/Li ratio.

Dopamine is a low-molecular-weight catecholamine capable of self-polymerizing to form a poly(dopamine) (PDA) layer on both inorganic and organic materials [15,16]. The PDA layer on the substrate membrane surface improves the permeation flux and the interaction between PEI and the PDA layer by chemical bonds, which can enhance the stability and compatibility of the active layer and the substrate membrane [17–19]. Zhang et al. [20] prepared an NF membrane by adhesion of PDA followed by PEI grafting, and the resulted membrane exhibited a high rejection of cationic dye. Lv et al. [21] fabricated an NF membrane via co-deposition of PDA/PEI followed by crosslinking, and this membrane showed good rejection for multivalent cations (>90%) and good structural stability for ethanol. However, it would take at least 4 h for the deposition of PDA on the surface of the support membrane [21,22] and consume a large amount of cross-linker. Besides, the effect of PEI molecular weight on the separation performance remains unclear, and these membranes have rarely been used to treat mixed salt solutions and salt lake brines with a high Mg/Li ratio.

In our previous study, we found that the cross-linking between PEI and PDA occurred more easily in ethanol solution than in aqueous solution. We have focused on the rapid preparation of a positively charged NF membrane for the separation of Mg^{2+} and Li^+ from brine with a high Mg/Li ratio. PEI was introduced on the polyimide (PI) substrate membrane surface via grafting with PDA layer, followed by cross-linking in ethanol solution with epichlorohydrin (ECH) as the cross-linker to form an active layer. The effects of immersion time, the molecular weight of PEI, cross-linker concentration, and operating conditions, such as Mg/Li ratio, were investigated. A long-term filtration test was performed to investigate the separation stability of this composite NF membrane.

2. Experimental section

2.1. Materials

Fluorine-containing polyimide was purchased from Changchun Gaoqi Polyimide Material Co., Ltd. (Changchun, China). N,N-dimethylacetamide (DMAc, analytical reagent (AR)), PEI with a molecular weight (Mw) of 600, 1,800, 10,000, and 70,000 Da, dopamine hydrochloride (DA, 98%, AR), Tris(hydroxymethyl) aminomethane (Tris-HCl, AR), ECH (AR), sodium sulfate (Na_2SO_4, AR), magnesium sulfate ($MgSO_4$, AR), magnesium chloride hexahydrate ($MgCl_2{\cdot}6H_2O$, AR), potassium chloride (KCl, 99.99%, AR), and lithium chloride (LiCl, AR) were purchased from Aladdin Co., Ltd., (Shanghai, China). Polyethylene glycols (PEGs) with an Mw of 200, 400, and 600 Da, glucose (AR), sucrose (AR), raffinose (AR), ethanol (99.5%, AR), sodium hydroxide (NaOH, AR), HCl (AR), and 1,4-dioxane (DOX, AR) were purchased from Titan Polytron Technologies Inc., (Shanghai, China). All chemicals were used without further purification. Aqueous solutions were prepared with pure water obtained using a reverse osmosis membrane system (UPT-I-5T, China).

2.2. Membrane preparation

2.2.1. Preparation of PI substrates

PI flat-sheet membrane substrates were prepared by the non-solvent induced phase inversion method. PI fibers were dissolved in the solvent and stirred for 24 h at room temperature to obtain a homogeneous solution. After degassing for 24 h, the solution was cast on a smooth glass plate using a film applicator with a thickness of 200 μm, evaporated in the air for 30 s, and then immersed in a coagulation bath. After phase separation, the resulted membranes were rinsed thoroughly with pure water and then stored in pure water before modification. The composition of prepared membranes is listed in Table 1.

2.2.2. Surface cross-linking of PI membranes

The cross-linking on the surface of PI membranes is schematically shown in Fig. 1. Firstly, 2 g of DA was dissolved in 1 L of Tris-HCl buffer solution (pH = 8.5, 50 mM). Then, PI membranes prewetted with ethanol for 30 min were immersed in DA solution and shaken at 25°C ± 0.2°C. The as-prepared PI/PDA membranes were thoroughly washed with pure water, and then pure water was removed from the membrane surface using filter paper at room temperature. PEI and ECH were dissolved in ethanol with a predetermined concentration. After that, PI/PDA membranes were immersed in the above solution for 1 h at 70°C ± 0.2°C. Finally, the obtained PI/PDA/PEI membranes were rinsed several times with pure water and stored in pure water before use.

2.3. Characterization

All samples were dried in a vacuum oven at 80°C ± 0.2°C for 24 h before characterization.

2.3.1. Morphology

The morphologies of the cross-section and the surface of the membranes were observed by field emission scanning

Table 1
Composition of prepared PI membranes

Composition of casting solution (%)			Composition of coagulation bath (%)	
PI	DOX	DMAc	Pure water	Ethanol
14.0	21.5	64.5	80.0	20.0

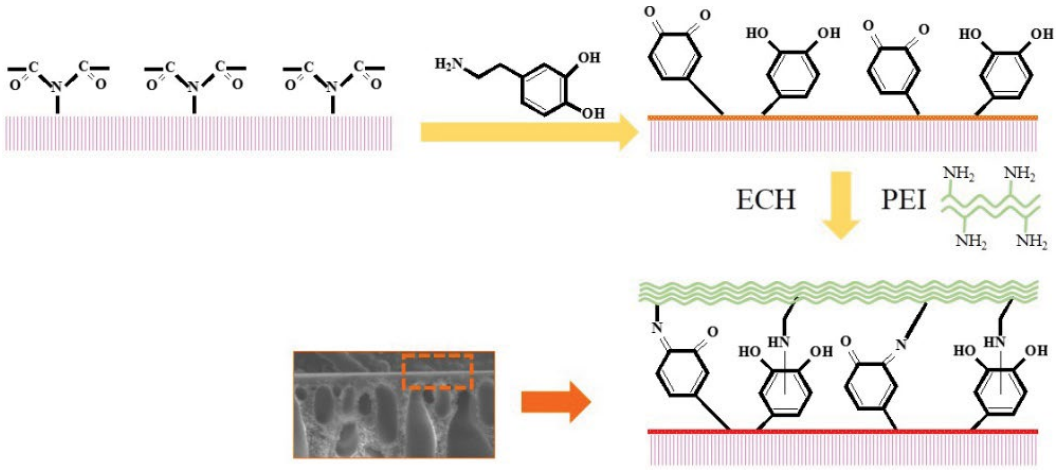

Fig. 1. Schematic of the surface cross-linking of PI membrane.

electron microscopy (SEM, S-4800, Japan). The surface roughness was analyzed by atomic force microscopy (AFM, Ntegra Prima, Russia), and 5 μm × 5 μm area was scanned by the tapping mode in air. Then, the root mean square roughness (Rms) and average roughness (Ra) were calculated.

2.3.2. Chemical structure and contact angle

The functional groups and elemental composition on the membrane surface were characterized by attenuated total reflection Fourier transform infrared spectroscopy (ATR-FTIR, Thermo Fisher 6700, USA) at a scanning wavenumber from 600 to 4,000 cm^{-1} and X-ray photoelectron spectroscopy (XPS, ESCALAB 250Xi, USA) with an Mg Kα photon energy of 1,253.6 eV, respectively. The hydrophilicity at five different positions in each sample was characterized by a contact angle goniometer (JC2000D2, China) at room temperature with 1.5 μL pure water as the droplet.

2.3.3. Zeta potential

The Zeta potential of the membrane surface was characterized by streaming potential measurement using the electrokinetic analyzer (SurPASS, Anton Paar, Austria) at 20°C ± 0.5°C with 1 mmol L^{-1} KCl solution as the electrolyte solution. The pH of the electrolyte solution was adjusted with 0.1 mol L^{-1} HCl or NaOH. All samples were immersed in 1 mmol L^{-1} KCl solution at room temperature for 4 h before measurement.

2.3.4. Molecular weight cutoffs of membranes

The MWCOs of membranes were tested using a variety of neutral solutes such as glucose, sucrose, raffinose, and PEGs (0.3 g L^{-1}) under 0.8 MPa. The concentration of neutral solutes before and after filtration was measured by a total organic carbon analyzer (TOC-VCPN, Shimadzu, Japan) and the rejection rate (R, %) was calculated by Eq. (1).

$$R = \left(1 - \frac{C_p}{C_f}\right) \times 100\% \tag{1}$$

where C_p and C_f are the concentration of permeate (g L^{-1}) and feed (g L^{-1}), respectively.

2.4. Membrane performance

The laboratory-scale cross-flow filtration module with an effective area of 35.3 cm^2 was used to test membrane performance (Fig. 2). The parameters of interest include the rejection rate and the volume permeate flux, which can be calculated by Eqs. (1) and (2), respectively. Before the experiment, each membrane was compacted with pure water at 0.5 MPa and 20°C ± 0.5°C for 30 min. Saline solutions (2.0 g L^{-1}), such as Na_2SO_4, $MgSO_4$, LiCl, and $MgCl_2$ were used as the feed solution. After testing, 10 mL of solution in the feed tank and the permeated solution were collected to measure salt concentration by an electrical conductivity meter (3100c, USA).

The volume permeate flux (J_v, L m^{-2} h^{-1}) is defined as the permeate solution volume per area per unit time.

$$J_v = \frac{V}{A\Delta t} \tag{2}$$

where V is the volume of permeate solution (L), A is the active surface area of the membrane (m^2), and Δt is the permeation time (h), respectively.

2.5. Separation of $MgCl_2$/LiCl

The selectivity of membranes was determined using simulated brine with different Mg/Li ratios prepared by inorganic salts with pure water and salt lake brine using the cross-flow filtration module, as shown in Table 2. The salt concentration (C_f) of both simulated brine and salt lake brine was 6.0 g L^{-1}.

SF (unitless) is a critical parameter describing the selectivity and separation efficiency of the membrane for the mixed salt solution, which is defined in Eq. (3).

$$\mathrm{SF} = \frac{\left(C_{\mathrm{Li}}^{+} / C_{\mathrm{Mg}}^{2+}\right)_{\mathrm{permeate}}}{\left(C_{\mathrm{Li}}^{+} / C_{\mathrm{Mg}}^{2+}\right)_{\mathrm{feed}}} \tag{3}$$

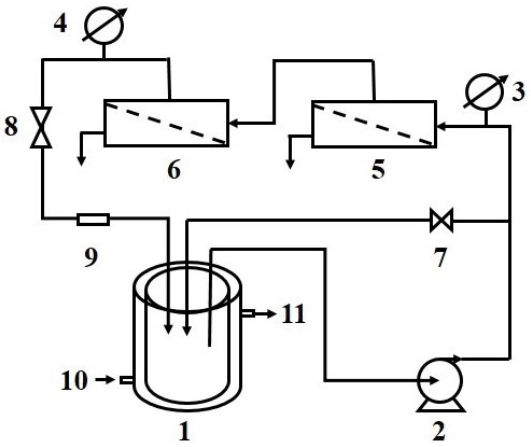

Fig. 2. Schematic of the cross-flow filtration module (1) feed tank, (2) pump, (3 and 4) pressure gauge, (5 and 6) membrane module, (7 and 8) valve, (9) flow meter, (10) circulating water inlet, (11) circulating water outlet.

Table 2
pH and ion concentrations of salt lake brine (g L^{-1})

pH	6.5
Na^+	1.345
K^+	0.591
Li^+	1.835
Ba^{2+}	0.001
Ca^{2+}	0.076
Mg^{2+}	119.800
Mg/Li	65.3

where C^{2+}_{Mg} and C^{+}_{Li} are the Mg^{2+} and Li^+ concentrations in permeate (g L^{-1}) and feed (g L^{-1}), respectively. Cation concentrations were determined by atomic absorption spectroscopy (HlTACHI-ZA3000, Japan). The pH of the solution was measured using a FE20K pH meter (Mettler Toledo, Swiss). The average values with standard deviations were calculated from at least three samples.

3. Results and discussion

3.1. Effects of fabrication conditions on the membrane performance

3.1.1. Molecular weight of PEI

The rejection of $MgCl_2$ and pure water flux for NF membranes with various molecular weights of PEI are shown in Fig. 3. It is noted that the rejection of $MgCl_2$ increases and the pure water flux decreases with increasing molecular weight of PEI, because membranes with a higher molecular weight of PEI have more terminal amino groups and thus can react more efficiently with PDA and cross-link with each other, resulting in the formation of a denser active separation layer on the surface. However, there is no difference in rejection of $MgCl_2$ (93.1% and 93.4%) and pure water flux (5.2 and 5.1 L m^{-2} h^{-1}) between membranes with a PEI molecular weight of 10,000 and 70,000 Da, indicating that PEI with a molecular weight of 10,000 Da has sufficient amino groups to react with PDA. In order to obtain a membrane with an excellent rejection rate and water flux, the mixed solution with different Mw of PEIs was used. Fig. 4 shows the effect of the ratio of PEI 600 to PEI 10,000 on the rejection of $MgCl_2$ and pure water flux. It is seen that the rejection of $MgCl_2$ increases continuously, but the pure water flux first decreases and then increases with the decrease of the ratio of PEI 600 to PEI 10,000, which can also be attributed to the formation of the denser active layer. Thus, it is not feasible to obtain an NF membrane with good performance from the mixing solution of PEIs, and PEI 10,000 is chosen to prepare the NF membrane.

Fig. 5 shows the surface and cross-sectional morphologies of membranes with different molecular weights of PEIs. Compared with the initial PI membrane, a thin and dense active layer is formed on the support PI membrane and the surface of PI/PDA/PEI membranes becomes denser with the increase of PEI molecular weight, indicating that Michael addition or Schiff base reactions have occurred and a cross-linked layer has been successfully fabricated on the surface of membranes [21,23].

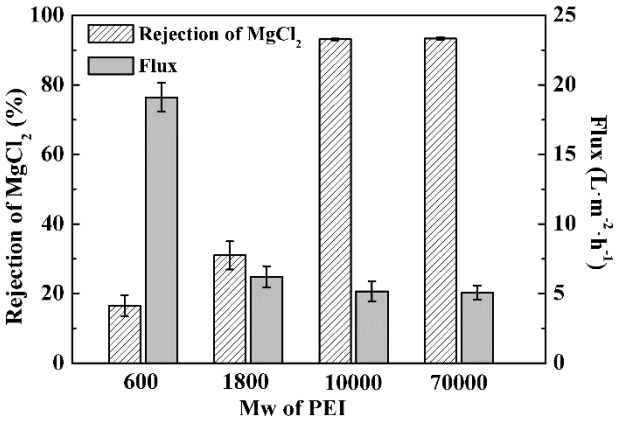

Fig. 3. Effect of PEI molecular weight on the membrane rejection of $MgCl_2$ and pure water flux (0.8 MPa).

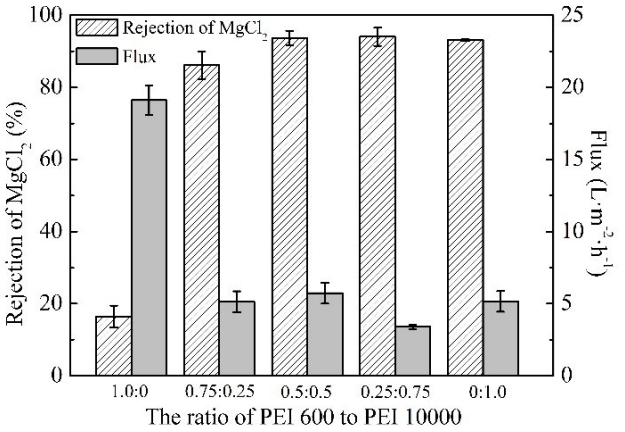

Fig. 4. Effect of the ratio of PEI 600 to PEI 10,000 on the membrane rejection of $MgCl_2$ and pure water flux (0.8 MPa).

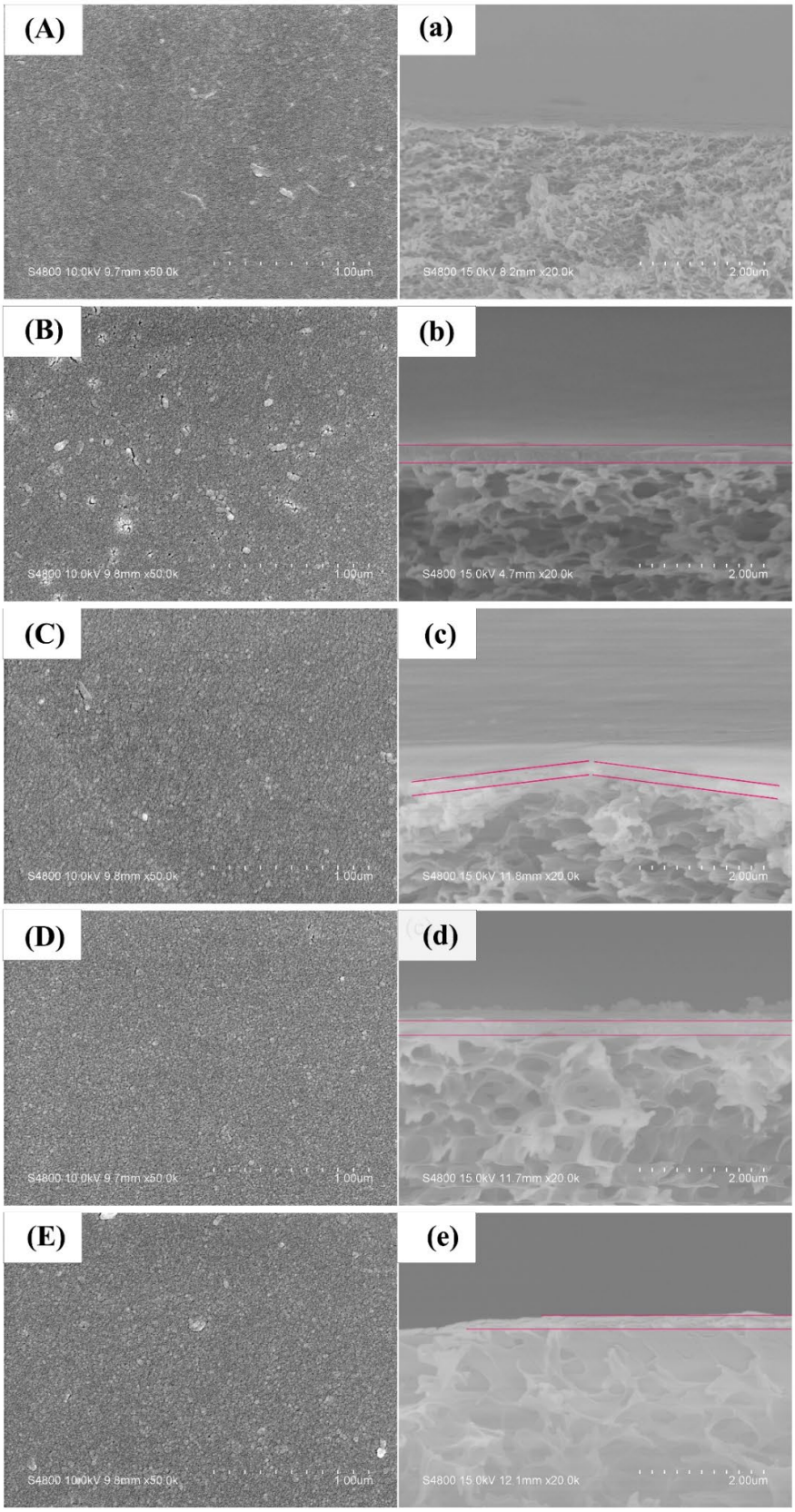

Fig. 5. SEM images of the surface and cross-sectional morphology of initial PI membrane (A, a) and PI/PDA/PEI membranes with different molecular weights of PEIs: 600 Da (B, b), 1,800 Da (C, c), 10,000 Da (D, d), and 70,000 Da (E, e).

3.1.2. DA deposition time and concentration of ECH

The effects of DA deposition time and ECH concentration on the membrane performance were investigated using 2.0 g L^{-1} inorganic salt ($MgCl_2$, $MgSO_4$, Na_2SO_4, and LiCl) solutions as the feeding solution in a cross-flow apparatus at 0.8 MPa and 20°C ± 0.5°C. Fig. 6a shows that the salt rejection follows the order of $MgCl_2$ > $MgSO_4$ > Na_2SO_4 > LiCl, which can be explained by Donnan exclusion, sieving, and transport principles. According to Donnan exclusion principle, the positively charged NF membrane has lower rejections for low-valence cations and high-valence anions than high-valence cations and low-valence anions, respectively [24,25]. The sieving and transport principles show that SO_4^{2-} has larger hydrated ionic radii (0.38 nm) and lower diffusion coefficient (1.065 × 10^{-5} cm^2 s^{-1}) than Cl^- (0.33 nm and 2.032 × 10^{-5} cm^2 s^{-1}) [24,26]. As the DA deposition time increases from 0.5 to 5.0 h, the pure water flux decreases from 5.0 to 1.8 L m^{-2} h^{-1} due to the blockage of membrane pores by the dense PEI cross-linked PDA layer, but the rejection rate of $MgCl_2$ increases from 22.2% to 91.7%. With the increase of DA deposition time, more PDA is attached to the membrane surface and thus the PDA layer becomes thicker, resulting in more reaction sites for PEI cross-linking and thus the formation of a denser cross-linked layer. Nevertheless, the pure water flux and inorganic salt rejections change little as the DA deposition time exceeds 2 h, illustrating that co-deposition of PDA/PEI reaches a stable state [21]. Thus, the optimum DA deposition time is determined to be 2 h.

The effect of ECH concentration (0.5%–1.5%) on the membrane performance was investigated. It can be seen from Fig. 6b that with the increase of ECH concentration, the pure water flux first increases slightly and then decreases; but the rejection of all inorganic salts shows only a gentle increase, which is attributed to the increased thickness of PEI cross-linked PDA layer. Thus, the optimum concentration of ECH is determined to be 1.0%.

3.2. Characterization of PI and cross-linked PI membranes

3.2.1. ATR-FTIR and XPS spectra of membrane surface

The chemical structures of membrane surfaces were characterized by ATR-FTIR and XPS. Fig. 7 shows the ATR-FTIR spectra of PI substrate, PI/PDA membrane, and PI/PDA/PEI membrane. In addition to typical PI bands of the substrate, two new peaks are observed at 3,367 and 1,532 cm^{-1} in PI/PDA and PI/PDA/PEI membranes, which correspond to the N–H stretching vibration of PDA and PEI, respectively [20,21], and their relative intensities are significantly increased in the spectrum of PI/PDA/PEI membrane. These characteristic bands suggest that PDA and PDA/PEI composite layers have been successfully formed on the PI substrate.

The XPS spectra and the relative elemental content of initial PI membrane, PI/PDA membrane, and PI/PDA/PEI

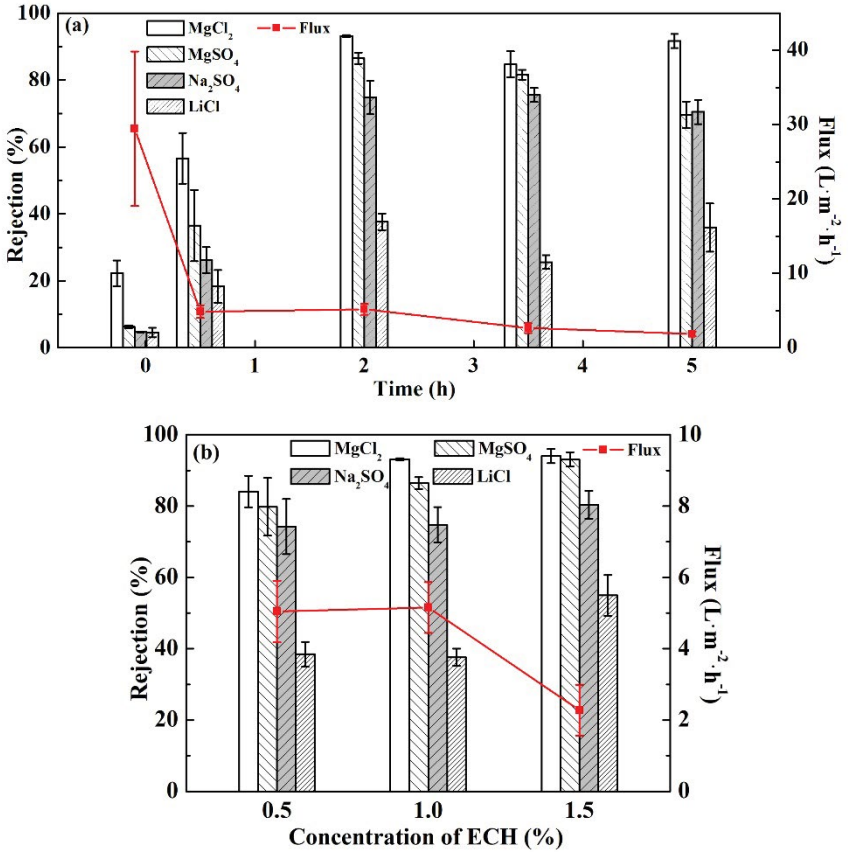

Fig. 6. Effect of DA deposition time (a) and ECH concentration (b) on membrane performance.

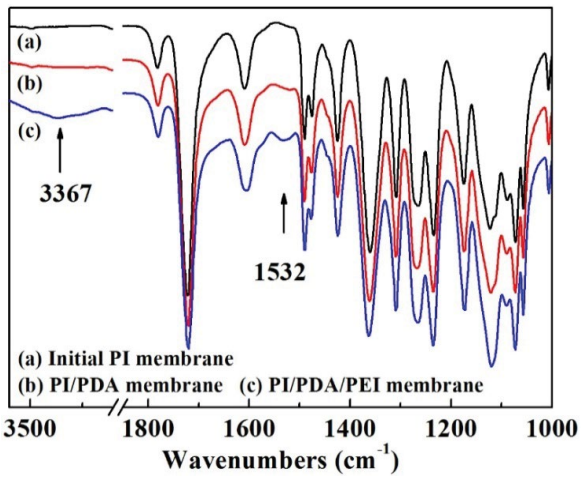

Fig. 7. ATR-FTIR spectra of the initial PI membrane (a), PI/PDA membrane (b), and PI/PDA/PEI membrane (c).

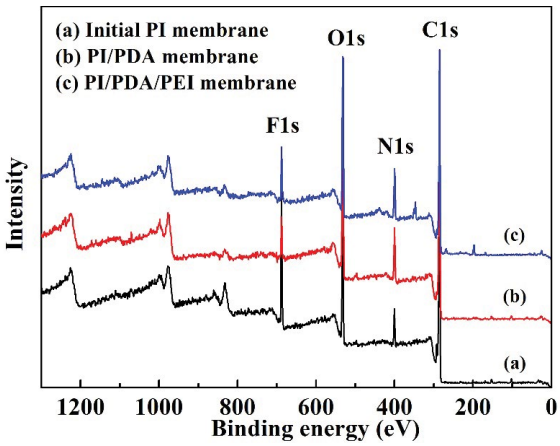

Fig. 8. XPS spectra of the initial PI membrane (a), PI/PDA membrane (b), and PI/PDA/PEI membrane (c).

membrane are shown in Fig. 8 and Table 3. Four major emission peaks are identified at 688, 532, 400, and 285 eV corresponding to F_{1s}, O_{1s}, N_{1s}, and C_{1s}, respectively. Compared with the initial PI membrane, the PI/PDA membrane shows an increase in N and O elements but a decrease in F element due to the high percentage of O and N elements in PDA. The content of N element and the atomic ratio of N/C are further increased from 8.47% and 0.13 to 10.39% and 0.16 for the PI/PDA/PEI membrane after PEI cross-linking, respectively, which may be derived from the high percentage of N element in PEI. Thus, PEI has been successfully anchored onto the PDA layer to form a dense surface of amine groups.

3.2.2. Hydrophilicity of membranes

Surface hydrophilicity is a critical parameter affecting the permeate flux and anti-fouling performance of membranes. In order to evaluate the hydrophilicity of membranes more accurately, the dynamic contact angle was measured. As shown in Fig. 9, the contact angle of the initial PI membrane is 77°, which is obviously higher than that of PI/PDA membrane (53°) and PI/PDA/PEI membrane (61°) prepared under optimum conditions. The PI/PDA membrane exhibits the best wettability and its water contact angle decreases from 53° to 42° within 110 s, indicating that a highly hydrophilic PDA layer has been formed on the surface of PI membrane. It is noteworthy that the contact angle of PI/PDA/PEI membrane increases slightly after

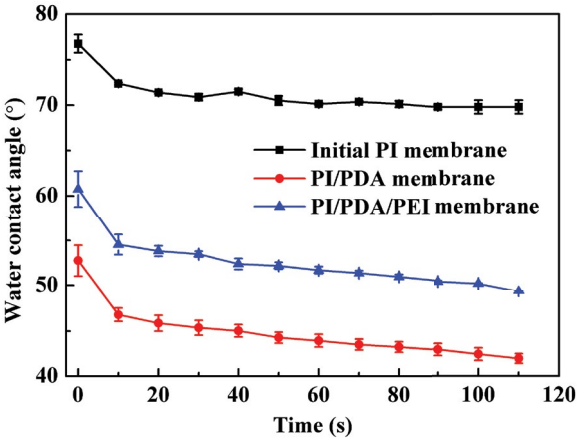

Fig. 9. Contact angles of the initial PI membrane, PI/PDA membrane, and PI/PDA/PEI membrane.

cross-linking of PEI, which may be attributed to the difference of hydrophilicity between PEI and PDA [17]. However, the hydrophilicity of PI/PDA/PEI membrane is still superior to that of the initial PI membrane.

3.2.3. Surface morphology and roughness of membranes

Fig. 10 and Table 4 show the surface SEM images, corresponding 3D AFM images, and surface roughness of initial PI membrane, PI/PDA membrane, and PI/PDA/PEI membrane.

Table 3
Relative elemental content on surface of initial PI membrane, PI/PDA membrane, and PI/PDA/PEI membrane

Membrane	Relative elemental content (at %)				Atomic ratio
	C	N	O	F	N/C
Initial PI membrane	66.40	5.38	18.87	9.35	0.08
PI/PDA membrane	66.75	8.47	21.88	2.90	0.13
PI/PDA/PEI membrane	64.39	10.39	19.83	5.39	0.16

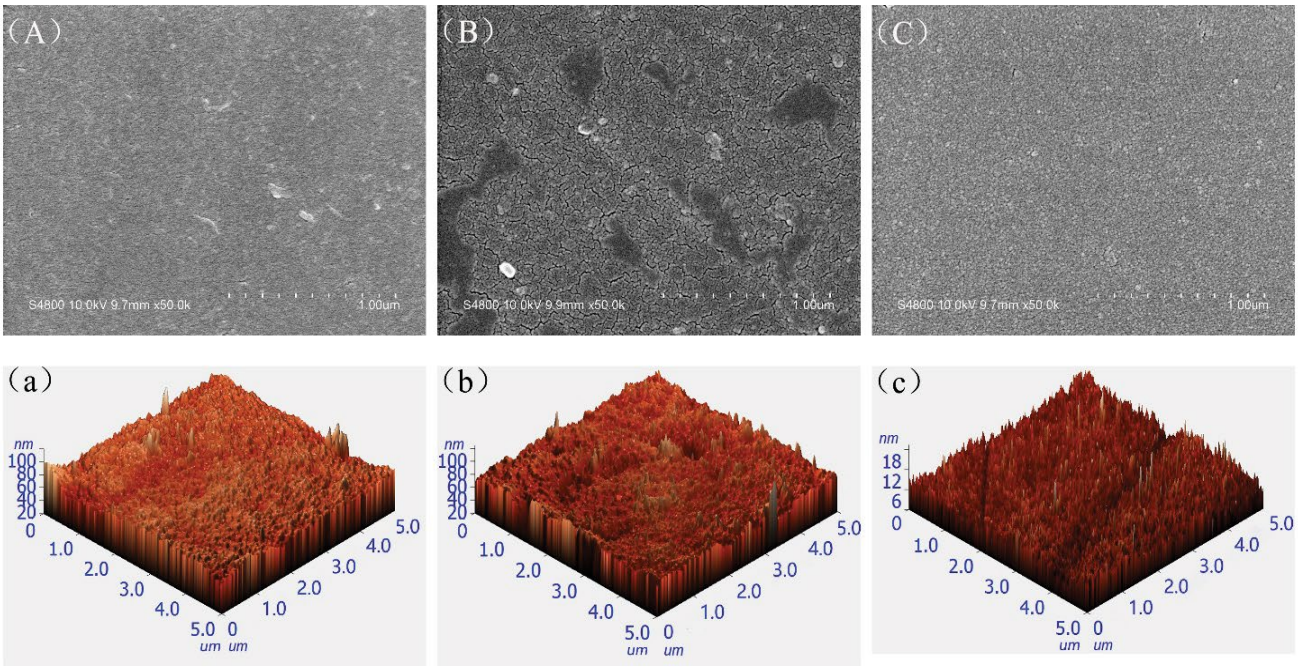

Fig. 10. SEM and AFM images of membranes. (Surface morphology (A–C) and AFM image (a–c) of the initial PI membrane, PI/PDA membrane, and PI/PDA/PEI membrane, respectively).

Table 4
Surface roughness of initial PI membrane, PI/PDA membrane, and PI/PDA/PEI membrane

Membranes	Ra (nm)	Rms (nm)
Initial PI	3.361	4.485
PI/PDA	5.050	7.153
PI/PDA/PEI	1.412	1.793

It can be seen that the roughness of membranes follows the order of PI/PDA membrane > initial PI membrane > PI/PDA/PEI membrane, which can be caused by the deposition of loose aggregates of PDA on the membrane surface. After cross-linking of PEI, Ra and Rms of PI/PDA/PEI membrane are decreased to 1.412 and 1.793 nm, respectively, indicating that the membrane surface becomes smoother and denser compared to the initial PI membrane and PI/PDA membrane.

3.2.4. Zeta potential of membranes

The zeta potential of the initial PI membrane and PI/PDA/PEI membrane is shown in Fig. 11. The isoelectric points of the initial PI membrane and PI/PDA/PEI membrane are pH = 4.68 and 6.95, respectively, indicating that the PI/PDA/PEI membrane is positively charged at pH < 6.95 due to the protonation of amine groups [20,27]. Therefore, for the PI/PDA/PEI membrane, electrolyte solutes with higher cationic charged densities and/or with lower anionic charged densities are rejected more effectively [28]. Generally, the NF membrane is used at pH = 6.0 [21,29], and thus PI/PDA/PEI membrane is positively charged during the NF operation process.

3.2.5. Molecular weight cutoff of membranes

The MWCO of membranes is used to characterize their pore sizes, which is obtained by the molecular weight when the rejection of neutral solutes reaches 90% [30]. Fig. 12 shows the rejection curves of PI/PDA/PEI membrane to glucose, sucrose, raffinose, and PEGs. It shows that the MWCO of PI/PDA/PEI membrane is about 449 Da, indicating that this membrane is an NF membrane [6–8].

3.3. Separation performance of PI/PDA/PEI membrane

The separation performance of the PI/PDA/PEI membrane is evaluated using $MgCl_2$/LiCl solutions and salt lake brine. The salt lake brine in China typically has a wide range of Mg/Li ratios. Fig. 13 shows that the rejection of Mg^{2+} is maintained at about 89.0% with the increase of the Mg/Li ratio, but that of Li^+ increases with the increase of the Mg/Li ratio. Therefore, the Mg/Li ratio of permeate increases with increasing Mg/Li ratio of feeding solution, but it is much lower than that of feeding solution.

To investigate the separation stability of PI/PDA/PEI membrane, a 20 h filtration experiment was conducted using salt lake brine obtained from West Taijnar salt lake in China. Fig. 14 shows that the SF is maintained at 11.4 and the Mg/Li ratio decreases from 65.3 of the feeding solution to 5.0 of permeate solution, indicating that PI/PDA/PEI membrane has good separation performance and stability for Mg^{2+} and Li^+.

Compared with other NF membranes fabricated by PDA and PEI [17,20,21], less time is required for the fabrication of PI/PDA/PEI and better salt rejection is obtained in this study.

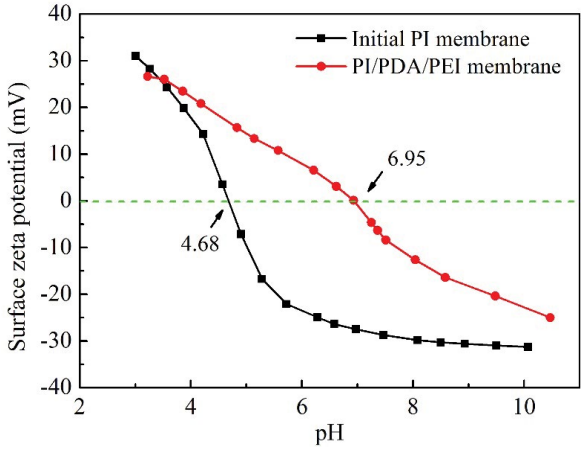

Fig. 11. Zeta potential of the initial PI membrane and PI/PDA/PEI membrane.

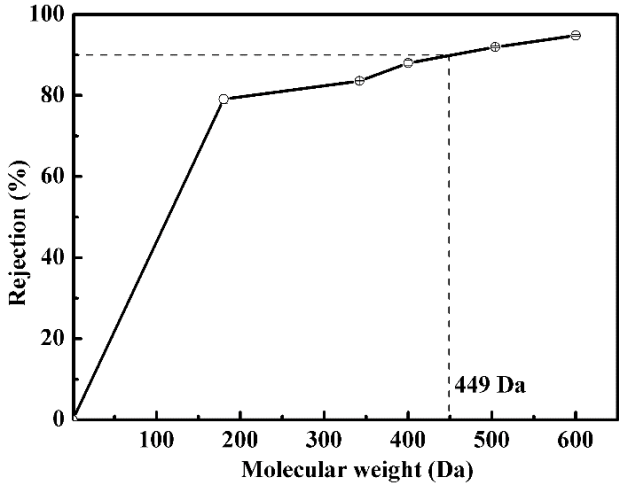

Fig. 12. Rejection curves of neutral solutes for PI/PDA/PEI membrane.

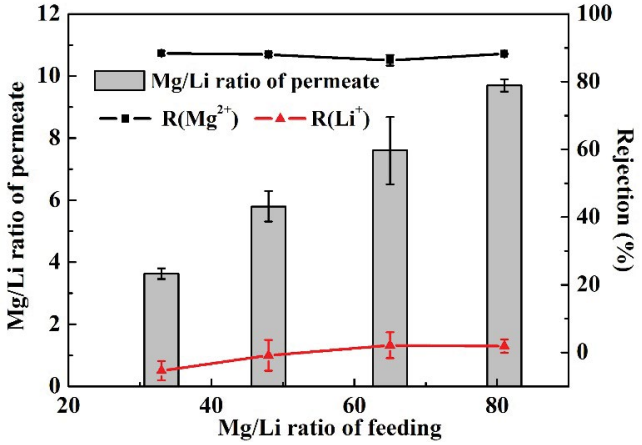

Fig. 13. Effect of Mg/Li ratio on the separation performance of PI/PDA/PEI membrane.

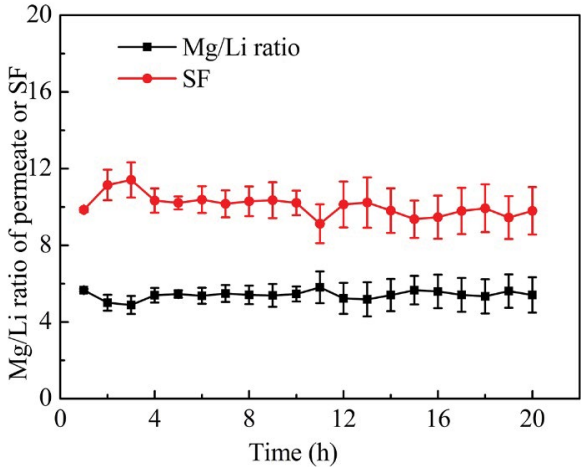

Fig. 14. Separation performance of PI/PDA/PEI membrane for 20 h filtration: Mg/Li ratio of permeate and SF.

4. Conclusions

A positively charged NF membrane was prepared in this study by cross-linking between PEI and PDA on the PI support membrane for separating Mg^{2+} and Li^{+} from $MgCl_2$/LiCl mixed solution with a wide range of Mg/Li ratios, and it took only 2 h for PDA deposition. The composite membrane shows excellent long-term stability and separation performance for brine with a high Mg/Li ratio, and the Mg/Li ratio of the permeate of brine obtained from West Taijnar salt lake can be reduced from 65.3 to 5.0 at pH 6.5 by filtration. The membrane has great potential for recovering Li resources from salt lake brine with a high Mg/Li ratio.

Acknowledgments

This research is financially supported by the National Natural Science Foundation of China (21764011), the Foundation from Qinghai Science and Technology Department (2020-HZ-808), and Thousand Talents Program of Qinghai Province.

Symbols

A	—	Active surface area of membrane, m^2
C_f	—	Concentration in feed, g L^{-1}
C_{Li+}	—	Concentration of Li^+, g L^{-1}
C^{2+}_{Mg}	—	Concentration of Mg^{2+}, g L^{-1}
C_p	—	Concentration in permeate, g L^{-1}
J_v	—	Volume permeate flux, L m^{-2} h^{-1}
R	—	Rejection rate, %
SF	—	Separation factor, unitless
V	—	Volume of permeate solution, L
Δt	—	Permeation time, h

References

[1] B. Ammundsen, J. Paulsen, Novel lithium-ion cathode materials based on layered manganese oxides, Adv. Mater.,13 (2001) 943–956.
[2] J.W. An, D.J. Kang, K.T. Tran, M.J. Kim, T. Lim, T. Tran, Recovery of lithium from Uyuni salar brine, Hydrometallurgy, 117–118 (2012) 64–70.

[3] G.P. Zhang, W. Qin, Y.Z. Tan, Y.Y. Dai, Separation of magnesium and lithium by solvent extraction using di-(2-ethylhexyl) phosphoric acid (D2EHPA), J. Tsinghua Univ. Sci. Technol., 50 (2010) 430–433.
[4] G.P. Xiao, K.F. Tong, L.S. Zhou, J.L. Xiao, S.Y. Sun, P. Li, J.G. Yu, Adsorption and desorption behavior of lithium ion in spherical PVC-MnO_2 ion sieve, Ind. Eng. Chem. Res., 51 (2012) 10921–10929.
[5] X.M. Wen, P.H. Ma, C.L. Zhu, Q. He, X.C. Deng, Preliminary study on recovering lithium chloride from lithium-containing waters by nanofiltration, Sep. Purif. Technol., 49 (2006) 230–236.
[6] X.L. Wang, T. Tsuru, M. Togoh, S. Nakao, S. Kimura, Evaluation of pore structure and electrical properties of nanofiltration membranes, J. Chem. Eng. Japan, 28 (1995) 186–192.
[7] X.L. Wang, T. Tsuru, S. Nakao, S. Kimura, The electrostatic and steric-hindrance model for the transport of charged solutes through nanofiltration membranes, J. Membr. Sci., 135 (1997) 19–32.
[8] B. Van der Bruggen, C. Vandecasteele, Removal of pollutants from surface water and groundwater by nanofiltration: overview of possible applications in the drinking water industry, Environ. Pollut., 122 (2003) 435–445.
[9] G. Yang, H. Shi, W.Q. Liu, W.H. Xing, N.P. Xu, Investigation of Mg^{2+}/Li^{+} separation by nanofiltration, Chin. J. Chem. Eng., 19 (2011) 586–591.
[10] A. Somrani, A.H. Hamzaoui, M. Pontie, Study on lithium separation from salt lake brines by nanofiltration (NF) and low pressure reverse osmosis (LPRO), Desalination, 317 (2013) 184–192.
[11] S.Y. Sun, L.J. Cai, X.Y. Nie, X. Song, J.G. Yu, Separation of magnesium and lithium from brine using a Desal nanofiltration membrane, J. Water Process Eng., 7 (2015) 210–217.
[12] X.H. Li, C.J. Zhang, S.N. Zhang, J.X. Li, B.Q. He, Z.Y. Cui, Preparation and characterization of positively charged polyamide composite nanofiltration hollow fiber membrane for lithium and magnesium separation, Desalination, 369 (2015) 26–36.
[13] W. Li, C. Shi, A. Zhou, X. He, Y.W. Sun, J.L. Zhang, A positively charged composite nanofiltration membrane modified by EDTA for LiCl/$MgCl_2$ separation, Sep. Purif. Technol., 186 (2017) 233–242.
[14] H.Z. Zhang, Z.L. Xu, H. Ding, Y.J. Tang, Positively charged capillary nanofiltration membrane with high rejection for Mg^{2+} and Ca^{2+} and good separation for Mg^{2+} and Li^{+}, Desalination, 420 (2017) 158–166.
[15] Q. Ye, F. Zhou, W.M. Liu, Bioinspired catecholic chemistry for surface modification, Chem. Soc. Rev., 40 (2011) 4244–4258.
[16] S. Hong, Y.S. Na, S. Choi, I.T. Song, W.Y. Kim, H. Lee, Non-covalent self-assembly and covalent polymerization co-contribute to polydopamine formation, Adv. Funct. Mater., 22 (2012) 4711–4717.
[17] M.M. Li, J. Xu, C.Y. Chang, C.C. Feng, L.L. Zhang, Y.Y. Tang, C.J. Gao, Bioinspired fabrication of composite nanofiltration membrane based on the formation of DA/PEI layer followed by cross-linking, J. Membr. Sci., 459 (2014) 62–71.
[18] S. Azari, L. Zou, Using zwitterionic amino acid L-DOPA to modify the surface of thin film composite polyamide reverse osmosis membranes to increase their fouling resistance, J. Membr. Sci., 401–402 (2012) 68–75.
[19] S.P. Sun, T. Alan Hatton, S.Y. Chan, T.S. Chung, Novel thin-film composite nanofiltration hollow fiber membranes with double repulsion for effective removal of emerging organic matters from water, J. Membr. Sci., 401–402 (2012) 152–162.
[20] R.N. Zhang, Y.L. Su, X.T. Zhao, Y.F. Li, J.J. Zhao, Z.Y. Jiang, A novel positively charged composite nanfiltration membrane prepared by bio-inspired adhesion of polydopamine and surface grafting of poly(ethylene imine), J. Membr. Sci., 470 (2014) 9–17.
[21] Y. Lv, H.C. Yang, H.Q. Liang, L.S. Wan, Z.K. Xu, Nanofiltration membranes via co-deposition of polydopamine-polyethylenimine followed by cross-linking, J. Membr. Sci., 476 (2015) 50–58.
[22] J. Sun, C.H. Wang, Y.Z. Wang, S.X. Ji, W.F. Liu, Immobilization of carbonic anhydrase on polyethylenimine/dopamine codeposited membranes, J. Appl. Polym. Sci., 136 (2019) 47784, doi: 10.1002/app.47784.
[23] F.Y. Zhao, Y.L. Ji, X.D. Weng, Y.F. Mi, C.C. Ye, Q.F. An, C.J. Gao, High-flux positively charged nanocomposite nanofiltration membranes filled with poly(dopamine) modified multiwall carbon nanotubes, Appl. Mater. Interfaces, 8 (2016) 6693–6700.
[24] J. Schaep, B. Van der Bruggen, C. Vandecasteele, D. Wilms, Influence of ion size and charge in nanofiltration, Sep. Purif. Technol., 14 (1998) 155–162.
[25] L.C. Li, B.G. Wang, H.M. Tan, T.L. Chen, J.P. Xu, A novel nanofiltration membrane prepared with PAMAM and TMC by in situ interfacial polymerization on PEK-C ultrafiltration membrane, J. Membr. Sci., 269 (2006) 84–93.
[26] D.R. Lide, CRC Handbook of Chemistry and Physics, CRC Press, Inc., Florida, USA, 2002, pp. 93–94.
[27] J. Xu, Z. Wang, J.X. Wang, S.C. Wang, Positively charged aromatic polyamide reverse osmosis membrane with high anti-fouling property prepared by polyethylenimine grafting, Desalination, 365 (2015) 398–406.
[28] S. Veríssimo, K.V. Peinemann, J. Bordado, Influence of the diamine structure on the nanofiltration performance, surface morphology and surface charge of the composite polyamide membranes, J. Membr. Sci., 279 (2006) 266–275.
[29] Y.C. Chiang, Y.Z. Hsub, R.C. Ruaan, C.J. Chuang, K.L. Tung, Nanofiltration membranes synthesized from hyperbranched polyethyleneimine, J. Membr. Sci., 326 (2009) 19–26.
[30] C.L. Liu, H.C. Mao, J.F. Zheng, S.B. Zhang, In situ surface crosslinked tight ultrafiltration membrane prepared by one-step chemical reaction-involved phase inversion process between activated PAEK-COOH and PEI, J. Membr. Sci., 538 (2017) 58–67.